Limnol. Oceanogr., 57(1), 2012, 221–234

doi:10.4319/lo.2012.57.1.0221

Nitrogen transformations in a through-flow wetland revealed using whole-ecosystem pulsed ^{15}N additions

Jonathan M. O'Brien,[a,1,*] Stephen K. Hamilton,[a,b] Lauren E. Kinsman-Costello,[a] Jay T. Lennon,[a,c] and Nathaniel E. Ostrom[b]

[a] W.K. Kellogg Biological Station, Michigan State University, Hickory Corners, Michigan
[b] Department of Zoology, Michigan State University, East Lancing, Michigan
[c] Department of Microbiology and Molecular Genetics, Michigan State University, Michigan

Abstract

We used pulsed and continuous additions of ^{15}N together with whole-ecosystem metabolism measurements to elucidate the mechanisms of nitrogen (N) transformations in a small (1170 m^2) through-flow wetland situated along a stream. From measurements of the wetland inflow and outflow, we observed a consistent decrease in nitrate (by 10% of inflow concentrations), while ammonium increased by an order of magnitude. Outflow ammonium concentrations oscillated in a diel cycle, inverse to the concentration of dissolved oxygen (i.e., greater ammonium export at night). The pulsed ^{15}N additions showed little uptake of nitrate over time in the wetland and rapid daytime uptake of ammonium from the water column (rate constant, $k_t = 0.11\ h^{-1}$). A steady-state ^{15}N-ammonium addition demonstrated a similar rate of ammonium uptake ($k_t = 0.067\ h^{-1}$), no detectable nitrification, and highlighted the spatial pattern of ammonium and nitrate uptake within the wetland. Porewater concentration profiles suggest high rates of net ammonium diffusion from the sediments. Ecosystem metabolism measurements indicate that release was attenuated during the day by autotrophic uptake, resulting in lower ammonium export during the day. Denitrification rates were modeled from dissolved N_2 : Ar ratios, but they were not sufficient to account for the observed loss in nitrate. Nitrate was removed near the pond inflow but not actively cycled throughout the pond, while the balance between sediment release and subsequent uptake of ammonium from the water-column dominated N cycling in this wetland.

Anthropogenic increases in the loading of nitrogen (N) to watersheds have led to increased N concentrations in groundwater, streams, and rivers, particularly in the form of nitrate (NO_3^-) (Böhlke 2002). This excess N contributes to eutrophication and impairment of inland and coastal surface waters (Rabalais 2002). Aquatic ecosystems along the flow path from terrestrial to marine environments, such as streams, lakes, rivers, and reservoirs, can have a large influence on N transport to coastal zones (Seitzinger et al. 2006; Alexander et al. 2009; Harrison et al. 2009). As water makes its way from landscapes into stream and river networks, often it passes through relatively lentic water bodies ranging from headwater wetlands to small impounded areas (e.g., beaver dams, mill ponds) to larger lakes and reservoirs. The longer water residence time in these lentic waters increases the influence of nutrient processing on the chemistry of through-flowing waters, and therefore these locations are potential 'hot spots' of nutrient processing.

Through-flow wetlands, defined here as wetlands through which water flows on its way to streams or other water bodies, are often situated at points of ground water discharge, serially along a stream's flow path, or parallel alongside streams and rivers. With their characteristically shallow depths and high rates of biological productivity, such wetlands typically function as sinks for excess nutrients in through-flowing water (Zedler 2003), which can be significant at the landscape level in watersheds where large quantities of water move through wetlands. Wetlands are particularly efficient sinks of NO_3^- (Saunders and Kalff 2001; Fairchild and Velinsky 2006), and the amount of wetland cover within watersheds can have a particularly strong influence on stream water NO_3^-, reducing N export from wetland-rich watersheds (Johnson et al. 1990). Small but abundant through-flow wetlands, including ponds and small impoundments along streams, may play a disproportionate role in cumulative N transformations within a watershed. For example, Jansson et al. (1994) found that a single through-flow pond on the River Råån removed as much N as the entire upstream river network.

The net reduction in N as water passes through wetlands has often been described based on mass balance studies (Saunders and Kalff 2001), yet the processes responsible for N retention and their controls are not fully understood. Large spatial variability of N transformation processes within wetlands (Stanley and Ward 1997) and the inherent hydraulic complexity of flow through shallow and often vegetated waters (Lightbody et al. 2008) present challenges for scaling up from traditional point-based measurements of N processing rates. Furthermore, point-based measurements often entail incubation of sediments in the laboratory that can be questioned for their relevance to in situ rates (Groffman et al. 2005); although such laboratory incubations are valuable in a comparative sense.

Whole ecosystem ^{15}N isotope addition techniques recently refined for headwater streams (Mulholland et al. 2008) could yield new insights into the processing of N in

* Corresponding author: jon.obrien@canterbury.ac.nz

[1] Present address: School of Biological Sciences, University of Canterbury, Christchurch, New Zealand

hydrologically complex aquatic ecosystems, but so far there have been only a few applications within wetlands (Tobias et al. 2003; Gribsholt et al. 2005; Erler et al. 2010). Tracer addition experiments using ^{15}N have demonstrated the importance of in-stream processes (assimilation and denitrification) in reducing N export from watersheds (Peterson et al. 2001; Mulholland et al. 2008). However the methods commonly used in stream studies require continuous isotope tracer addition for long periods that approach steady-state in tracer ^{15}N fluxes. In wetlands that have longer residence times than streams, obtaining steady-state in ^{15}N fluxes may be prohibitively expensive, and the protracted time to reach steady-state allows for complex secondary transformations of the added ^{15}N that potentially obfuscate interpretation of the results.

In this study of N processing in a shallow through-flow wetland, we take an alternative approach to steady-state isotope tracer additions, employing short-term pulsed ^{15}N isotope additions to elucidate mechanisms of N processing. We sought to identify the processes responsible for observed NO_3^- loss and ammonium (NH_4^+) production between the inflow and the outflow, a pattern that is common in through-flow wetlands (Fairchild and Velinsky 2006). Nitrogen isotope additions were conducted to examine the biotic transformations of available N forms as stream water moved through the wetland. Separate, discrete pulses of ^{15}N tracer in the form of nitrate ($^{15}NO_3^-$) or ammonium ($^{15}NH_4^+$) were used to examine turnover of water column inorganic N in the wetland. A continuous steady-state addition of ammonium ($^{15}NH_4^+$) was then used to further elucidate N transformations. Whole-ecosystem estimates of metabolism implicate autotrophic N assimilation as a strong NH_4^+ sink during the day. Our results show the relative importance of denitrification, remineralization, and assimilatory processes, and they demonstrate how short-term pulsed additions can reveal N cycling in wetlands and other water bodies that are prohibitively large and to hydraulically complex for steady-state tracer additions.

Methods

Study site—The study was conducted on a through-flow wetland located at Michigan State University's Kellogg Experimental Forest in southwestern Michigan. The site was selected because of its small size and readily measurable inflow and outflow, which allowed us to employ our pulsed ^{15}N addition technique as well as the steady-state approach. The wetland (specifically referred to here as 'the pond') was originally constructed as a fishing pond. It receives inflow water via a pipe from nearby Augusta Creek and drains back to the creek via a concrete sill (Fig. 1). The pond is shallow (mean depth 0.9 m), has an area of 1170 m^2, and normally does not thermally stratify. A considerable amount of fine organic detritus enters the pond from August Creek and settles out near the pond inflow, which over time has formed a shallow mucky delta over about a third of the pond area. During the summer, the pond supports growth of several species of submerged macrophytes (*Potamogeton* spp., *Ceratophyllum demersum, Myriophyllum* sp.) and filamentous algae (particularly *Oedogonium*) growing as metaphyton.

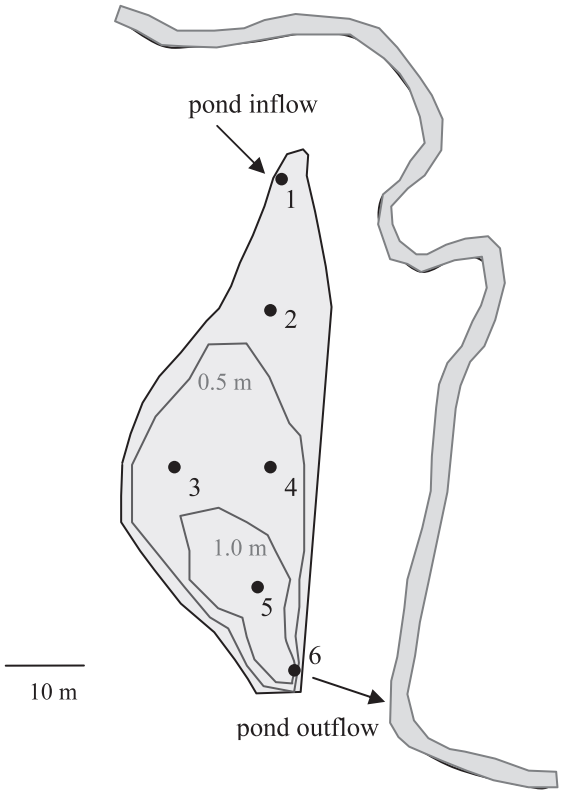

Fig. 1. Diagram of the Kellogg Forest Pond in relation to Augusta Creek, from which water is diverted through the pond. Depth contours are included.

Field measurements—We used a variety of field approaches to investigate the pattern of N transformation in the pond (i.e., loss of NO_3^- and gain of NH_4^+ in through-flowing waters). By employing multiple approaches, we were able to take advantage of synergies in the data, increasing our understanding beyond the results of any one method. We used diurnal mass balances and pulsed $^{15}NO_3^-$ and $^{15}NH_4^+$ additions to determine the gross fluxes of N cycling in the pond as a whole. A steady-state $^{15}NH_4^+$ addition then added spatial resolution to pattern of N transformation. Next, we used measurements of ecosystem metabolism, denitrification, and sediment porewater profiles to test the biological and physical mechanisms of N transformation. The advantage of employing multiple metrics in this way is that we gain greater level of inference and can better understand the mechanisms behind the pattern of N transformation.

Pulsed and steady-state ^{15}N additions—The ^{15}N pulse experiments consisted of the addition of tracer ^{15}N as either $^{15}NH_4^+$ or $^{15}NO_3^-$ to the pond inflow over a short period of time, followed by monitoring the export of tracer ^{15}N at the outflow. N uptake was estimated from the differential retention of the pulse of tracer ^{15}N relative to the conservative dye rhodamine WT dye (Ben Meadows, Co.) that was added with the tracer ^{15}N. Uptake rate constants

(k_t, h^{-1}) were then calculated from the pulses as a function of time within the pond.

Prior to the isotope pulse additions, we conducted a pulsed addition of RWT to determine mean hydraulic retention time and residence time distribution for the pond so that we could appropriately plan our sampling strategy. We calculated the mass of isotope for the pulse as (desired atom % enrichment) × (average N concentration) × (pond volume). Sampling at the pond outflow was planned to document the initial rising limb and peak of the ^{15}N pulse, followed by periodic sampling of the long declining tail until tracer ^{15}N reached relatively low abundance.

In the first experiment in late August 2007, a pulse of $^{15}NO_3^-$ and RWT was released at the pond inflow and ^{15}N abundance was monitored as a function of time at the pond outflow to determine NO_3^- uptake from the water column. A 7-liter solution of $^{15}NO_3^-$ and dye (24.6 mmol L^{-1} $^{15}NO_3^-$, 0.83 g L^{-1} RWT) was pumped into the pond inflow at 500 mL min^{-1} for 14 min (the pulse raised inflow NO_3^- concentrations by 10%). Samples for analysis of RWT and dissolved N species were collected using an automated ISCO 3700 water sampler (Teledyne Isco, Inc) on an hourly basis at the pond outflow. The pond inflow and outflow were sampled 10 times over the experiment to measure net changes in $^{15}NO_3^-$ abundance and NO_3^- and NH_4^+ concentrations and to verify that concentration changes during storage of samples in the automated sampler were inconsequential. Additionally, several samples were collected along the leading edge and tail of the tracer pulse at the pond outflow to measure incorporation of ^{15}N from NO_3^- into $^{15}NH_4^+$.

A similar pulse of $^{15}NH_4^+$ and RWT was released into the pond inflow to examine NH_4^+ uptake in early September 2007. A 7 L solution of ^{15}N and dye (10.1 mmol L^{-1} $^{15}NH_4^+$, 0.63 g L^{-1} RWT) was added to the pond inflow in a similar manner to the $^{15}NO_3^-$ pulse. Inflow and outflow water samples were collected 12 times during the experiment to measure $^{15}NH_4^+$ concentration as well as incorporation of ^{15}N into $^{15}NO_3^-$. Samples for RWT, NH_4^+, and NO_3^- were also collected by the automated water sampler hourly at the pond outflow.

A steady-state addition of $^{15}NH_4^+$ and RTW was conducted 2 weeks after the $^{15}NH_4^+$ pulse, starting September 2007. The purpose of this continuous isotope addition was to allow us to examine the spatial pattern of NH_4^+ uptake within the pond and to provide a comparison with the results of the pulsed addition. A solution of tracer ^{15}N and RWT was dripped into the pond inflow (0.3 μmol s^{-1} $^{15}NH_4^+$, 45 μg s^{-1} RWT) for 36 h in order to reach a steady-state plateau of RWT concentration. We collected water samples at the inflow and outflow as well as at four sites within the pond itself (Fig. 1). Samples for RWT were collected at two depths (0.1 m and 0.5 m) at all six locations during the rising limb of the continuous tracer addition to determine mean water travel times for each site. Samples for determination of RWT, NO_3^-, NH_4^+, and $^{15}NH_4^+$ were collected at all six sites after 24 h and 36 h (dawn and dusk) to examine nocturnal and diurnal differences in N processing. As with the pulsed ^{15}N experiments hourly samples were collected at the pond outflow.

We used RWT as a conservative tracer in this study in spite of evidence that under some circumstances sorption and photo-degradation may cause RWT to act nonconservatively, resulting in poor tracer recovery (Sutton et al. 2001). However, in wetlands with limited sediment–water exchange and short residence times (less than a week), recoveries are sufficient for RWT to be useful in studies of hydrologic residence (Lin et al. 2003). We found good recoveries at the outflow in our initial dye pulses on this pond which suggested that the behavior of RWT here was sufficiently conservative for our purposes.

Metabolism, porewaters, and denitrification—We estimated ecosystem metabolism from diel changes in dissolved oxygen (DO) concentration measured at the pond outflow using a Hydrolab data sonde, employing the one-station technique typically used in streams (Mulholland et al. 2004). Metabolism measurements were conducted during both ^{15}N pulses, during the continuous $^{15}NH_4^+$ addition and during the denitrification measurement. The sonde measured and logged DO at 15 min intervals. Air–water gas exchange coefficients for the pond were determined using the dark regression method (Young and Huryn 1999). The approach is based on the fact that at night, when there is no photosynthesis, the change in dissolved oxygen is a function of community respiration (CR) and reaeration, such that

$$dDO/dt = CR + K_{DO}(DO_t - DO_{equil}) \quad (1)$$

The reaeration coefficient (K_{DO}) and community respiration (CR) can be determined by linear regression of the rate of DO change (dDO/dt) and oxygen deficit ($DO_t - DO_{equil}$, or difference between ambient concentration at time t and the equilibrium DO concentration at the temperature of the water). We used hourly changes in DO and average DO deficits (between 23:00 h and 06:00 h) to calculate K_{DO} and CR. Reaeration coefficients were standardized to a temperature of 20°C ($K_{20} = K_{DO}\ 1.020^{-(t-20)}$). Gross primary production (GPP) was then calculated based on diurnal production of DO after correction for respiration and reaeration (using K_{20} adjusted for diurnal increases in temperature).

We used porewater equilibrators (Hesslein 1976), also known as peepers, to sample NH_4^+ and NO_3^- concentrations in porewaters in the upper 50 cm of pond sediments, allowing us to infer the N dynamics between the sediments and porewaters. Each peeper consisted of a tapered acrylic block (60 × 6.5 × 3.8 cm) with 14 pairs of wells drilled into it. The wells were covered with a Biotrans® Nylon membrane (MP Biomedical) and a thin acrylic faceplate, with cut-outs to match well openings. The peepers were assembled underwater and were deoxygenated by sparging with He overnight. We deployed the peepers at several locations in the pond by sinking them into the soft sediments until only the uppermost pair of wells remained above the sediment surface. Peepers were allowed to equilibrate with the sediment porewaters for 14 d. Porewater samples were removed from the wells using a syringe. Despite overnight degassing of the peepers with He, it is

possible for O_2 to diffuse slowly out of the plastic (Carignan et al .1994). This is unlikely to have had a large effect on our highly organic, anoxic sediments, but caution should be used when applying this technique in more oligotrophic systems.

As a follow-up to the isotope tracer-addition studies, we attempted to get a direct measure of denitrification in the pond using the open-system dissolved nitrogen to argon ratio (N_2 : Ar) technique (Laursen and Seitzinger 2002). In September 2009, we collected samples for determination of N_2 : Ar ratios at the pond inflow and outflow every 3 h for a period of 2 d. Water samples were transferred by syringe, taking care to avoid air contamination, to 12-mL Exetainer vials (Labco), preserved with 10 μL of saturated HgCl, capped without entrainment of bubbles, and stored in water-filled 50 mL centrifuge tubes until analysis using a membrane-inlet mass spectrometer by T. Kana at the University of Maryland's Horn Point Laboratory (Kana et al. 1994). A Hydrolab data sonde at the pond outflow monitored temperature and dissolved O_2. We added a pulse of RWT to the pond inflow to estimate residence time distribution.

Laboratory analyses—Surface water samples were analyzed for NH_4^+ using the phenol hypochlorite method (Aminot et al. 1997). Concentrations of NO_3^- (and, in porewater samples, NH_4^+) were measured using membrane-suppression ion chromatography with conductivity detection. Rhodamine WT concentrations were measured using a Turner Model 450 fluorometer (excitation filter: 540 nm, emission filter 585 nm).

The ^{15}N content of NO_3^- was determined by using a modified version of the diffusion method presented by Sigman et al. (1997). Water samples containing $\sim$ 50 μg NO_3^- − N were concentrated and NH_4^+ was removed by boiling with 3.0 g MgO and 5.0 g NaCl. Samples were then transferred to 250 mL media bottles to which an additional 0.5 g MgO, 0.5 g Devarda's alloy, and a Teflon filter packet were added. The Teflon filter packet was constructed by sealing a 10-mm Whatman GF/D glass-fiber filter, acidified with 25 μL of 2.0 M $KHSO_4$, within a packet made of two sealed Teflon filters. The sample NO_3^- was reduced to NH_4^+ by reacting at 60 °C for 48 h with DeVarda's alloy. Sealed bottles were then placed on a shaker for 7 d to allow for diffusion into the headspace and trapping on the acidified filter. The filter was then removed from the media bottle, dried, and analyzed for ^{15}N abundance using a Europa isotope-ratio mass spectrometer. A similar method was used to determine ^{15}N content of NH_4^+. Filtered water samples were transferred to 1-liter Nalgene polypropylene bottles to which 3.0 g MgO, 50 g NaCl, and a Teflon filter packet were added. Bottles were sealed and placed on a heated shaker for 14 d at 40°C to allow for diffusion and trapping on the filters. We used triplicate check samples (samples of known concentration) to test % recovery and precision for NO_3^- and NH_4^+ isotope samples (recovery > 98%).

Data analysis—The residence time distribution (RTD) of the pond was calculated from the concentration of dye tracer leaving the pond over time. The RTD is essentially the proportion of the solute mass that exits the pond at any given time and is calculated as (Danckwerts 1953)

$$\mathrm{RTD(t)} = \frac{\mathrm{QC(t)}}{\int_0^\infty \mathrm{QC(t)}d\mathrm{t}} = \frac{\mathrm{C(t)}}{\int_0^\infty \mathrm{C(t)}d\mathrm{t}} = \mathrm{C(t)Q/M} \qquad (2)$$

where C(t) is the RWT concentration at a given time, Q is the discharge, and M is the total mass of conservative tracer. From the RTD, we calculated the mean residence time (τ) as

$$\tau = \int_0^\infty \mathrm{tRTD(t)}d\mathrm{t} \qquad (3)$$

We estimate the net daily uptake of NO_3^- and the net daily production of NH_4^+ as the average difference between inflow and outflow concentrations, multiplied by throughflow discharge (measured with a velocity meter), integrated over a 24 h period, and divided by the pond area. To estimate the autotrophic component of NH_4^+ uptake, we assumed that the observed diel cycle in NH_4^+ concentrations at the outflow was primarily due to a balance of autotrophic assimilation and a constant rate of NH_4^+ production (*see* Results for rationale). We calculated the autotrophic uptake by integrating the diurnal NH_4^+ curve against the peak nighttime NH_4^+ concentration at the outflow (Johnson et al. 2006; Heffernan and Cohen 2010). Autotrophic N demand was calculated from the GPP using a photosynthetic quotient of 1.2 to convert molar O_2 production to CO_2 production, assuming an autotrophic net autotrophic production of 0.5 and an autotrophic C : N of 10. Total NH_4^+ production was then calculated as the peak nighttime NH_4^+ concentration at the outflow extended over 24 h.

We estimated gross uptake rates from the pulsed ^{15}N additions as the loss of tracer ^{15}N relative to the dye tracer. The abundance of the tracer ^{15}N was calculated from the sample $\delta^{15}N$ values corrected for background $\delta^{15}N$ (as measured in the inflow), converted to ^{15}N mole fractions, and multiplied by N concentrations as described in Mulholland et al. (2004 and 2008). Tracer ^{15}N abundance was predicted at the pond outflow based on the concentration of RWT and initial ratio of ^{15}N : RWT in the tracer solution. The observed tracer ^{15}N abundance at the pond outflow was divided by the predicted ^{15}N concentration to yield the proportion of ^{15}N remaining ($^{15}N_{obs}$: $^{15}N_{pred}$). The tracer ^{15}N uptake rate constant (k_t) was determined as the slope of ln-transformed $^{15}N_{obs}$: $^{15}N_{pred}$ over mean travel time. Comparisons were made in the main portion of the peak (3–15 h) to avoid ratio inflation in the tail due to detection limits (Dodds et al. 2008). Uptake rate constants during the steady-state $^{15}NH_4^+$ addition were determined by linear regression of the mean ln-transformed $^{15}N_{obs}$: $^{15}N_{pred}$ at each site within the pond on the site-specific mean travel time. Gross NH_4^+ uptake on an areal basis (mg m^{-2} h^{-1}) was calculated by multiplying k_t by pond NH_4^+ concentration (mg L^{-1}), and dividing by pond depth (m). Gross production of NH_4^+ was calculated by adding gross uptake and net production.

Table 1. Concentrations of NO_3^- and NH_4^+, discharge, and residence time (± SE) during the three tracer additions. Temperature is reported as daily mean temperature and range.

	NO_3^- (mg N L^{-1})		NH_4^+ μg N L^{-1})		Discharge ($L\ s^{-1}$) outflow	Temperature (°C)	Residence time (h)
	Inflow	Outflow	Inflow	Outflow			
$^{15}NO_3^-$ pulse	1.42(0.02)	1.29(0.04)	2.2(1.9)	25.9(13.9)	21(1.5)	20.5(22–19)	11.2
$^{15}NH_4^+$ pulse	1.60(0.06)	1.52(0.03)	0.0	31.6(7.9)	18(1.6)	16.3(14–17)	11.9
Continuous $^{15}NH_4^+$ addition	1.84(0.03)	1.53(0.04)	0.0	120.0(22.3)	22(1.9)	16.7(14–19)	11.5

Sediment NH+ diffusion form porewater profiles—We estimated diffusive NH_4^+ flux from the sediments using the equation (Berner 1980)

$$J_s = -\phi \times D_s \times \delta C/\delta x \quad (4)$$

where J_s is the diffusive flux, ϕ is the sediment porosity, D_s is the diffusive coefficient in sediment pore waters, and $\delta C/\delta x$ is the change in concentration over distance. We determined D_s based on the temperature corrected diffusive coefficient of NH_4^+ (Li and Gregory 1974), corrected for sediment tortuosity using $D_o : D_s$ values of 1.1 to 1.3 for freshwater sediments with a porosity of 0.85 (Maerki et al. 2004). We calculated sediment diffusive NH_4^+ flux assuming a mean sediment NH_4^+ concentration of 4.5 mg L^{-1} at a sediment depth of 1 cm with porosities of 0.69–0.86 (based on values measured in the pond).

Denitrification estimates from N_2 : Ar ratios—We modeled the N_2 : Ar data at the pond outflow to determine rates of N_2 transport, atmospheric exchange and production (denitrification). First, we modeled the concentration of the inert gas Ar at the outflow based on the inflow concentrations and residence-time distribution, as measured by the RWT pulse. Conceptually, the Ar concentration at the outflow reflects the mixing of different flow paths of water representing inflow of various times (where Z_{t-n} is the proportion of flow of a given age) multiplied by the concentration of Ar at the time it entered the pond through the inflow (i.e., $C_t = Z_{t-1} \cdot C_{t-1} + Z_{t-2} \cdot C_{t-2} + \ldots + Z_{t-n} \cdot C_{t-n}$) moderated by gas exchange between the pond and the atmosphere. Dissolved Ar in the inflow (stream) water varied with time under the influence of the diel temperature cycle (Laursen and Seitzinger 2005). The model accurately matched the observed variation in dissolved Ar concentration at the pond outflow so we applied the same technique to the N_2 : Ar ratio data with the addition of atmospheric exchange and denitrification terms to the model

$$\begin{aligned} N_2 : Ar_{out} = \Sigma(&Z_{t-1} \times N2 : Ar_{in\ t-1} + \ldots \\ &+ Z_{t-12} \times N2 : Ar_{in\ t-12}) \\ &- [K_{N2} \times (N_{2out} - N_{2equil})/ \\ &Ar_{out} + D_n/Ar_{out}](t - t_{t-1}) \end{aligned} \quad (5)$$

where $N_2 : Ar_{out}$ is the ratio at time t, N_{2out} and Ar_{out} are respective concentrations at time t, K_{N2} is the rate constant of air–water gas exchange (h^{-1}), N_{2equil} is the atmospheric equilibrium concentration at time t (varies with temperature), and D_n is the production of N_2 via denitrification (mmol L^{-1} h^{-1}). The model was fit using a range of K_{N2} values, and D_n was then fit by minimizing the sum of squares between observed and predicted values using the Microsoft Excel Solver function. We converted dissolved oxygen nighttime regression K_{20} estimates to K_{N2} using a conversion factor of 0.956. The model was constrained so that the denitrification term could not be negative.

Results

Hydraulic patterns—Residence time distributions indicate that flow patterns were not consistent with either a plug-flow (advection-dispersion) model typically seen in streams or with a constantly stirred reactor model commonly applied for ponds and lakes. Flushing time in the pond, based on pond volume and discharge (Monsen et al. 2002), was 13.4 h (ranged 12.7 h to 16.0 h). Mean residence times (τ) were shorter, around 11.5 h (Table 1). Residence time distributions indicated the leading edge of RWT reaching the pond outflow within three h, followed by peak concentration at ~ 4–5 h after the pulse addition and a long tail (Fig. 2). A consistent secondary peak occurred around 9–10 h indicating a distinct flow path within the pond. Thus there was evidently some short-

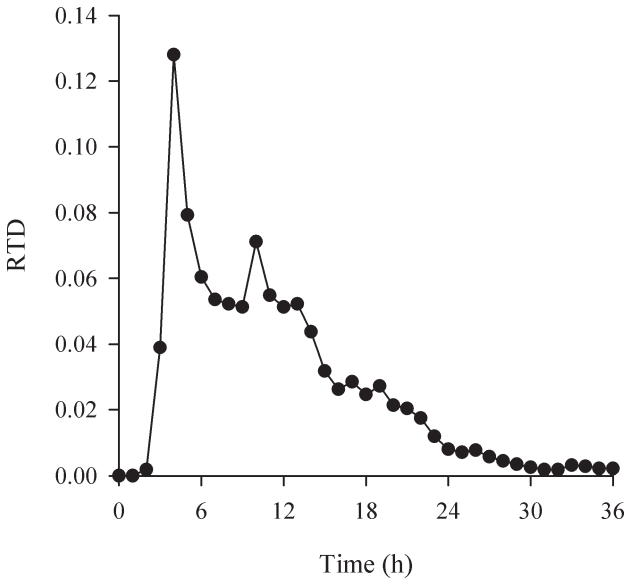

Fig. 2. Residence time distributions (RTD) for Kellogg Forest Pond based on tracer dye measurements at the pond outflow.

circuiting of flow as well as a more protracted movement of water through the pond.

Aquatic metabolism—Aquatic ecosystem metabolism had marked effects on DO concentrations in the pond. Although inflow DO concentrations remained fairly close to atmospheric equilibrium throughout the day, outflow concentrations generally varied between 65% to 110% of atmospheric equilibrium on a diel cycle. Gross primary production in the pond averaged 6.1 ± 2.0 g O_2 m^{-2} d^{-1} (mean ± SE) across all sampling dates, with highest rates in mid-September 2007. Community respiration in the pond averaged 16.0 ± 3.0 g O_2 m^{-2} d^{-1} across all sampling dates and rates were also highest in mid-September 2007. Gas exchange rate constants for dissolved O_2 (K_{20}, standardized to 20°C) were consistent across dates (0.29 ± 0.06 h^{-1}).

N processing—The pond was a consistent sink for NO_3^- and source of NH_4^+ during the period of study. Average inflow concentrations of NO_3^- across all three experiments were 1.62 mg N L^{-1}, while outflow concentrations were 10% lower at 1.45 mg N L^{-1} (Table 1) (*t*-test, $t = 12.67$, df = 11, $p < 0.001$). Outflow NO_3^- concentrations did not vary greatly over a 24 h cycle. Inflow concentrations of NH_4^+ were far lower than NO_3^- and mostly below our detection limit of ~ 3 μg N L^{-1}, however outflow NH_4^+ concentrations averaged 59 μg N L^{-1}. Outflow NH_4^+ concentrations varied considerably among dates and over a diel cycle, often varying by > 40% of the daily mean over 24 h (Fig. 3). SRP concentrations (mean, 6.5 μg L^{-1}) did not differ significantly between the pond inflow and outflow, and did not vary consistently over a 24 h cycle. Discharge did not differ between the pond inflow and outflow.

In the $^{15}NO_3^-$ pulse experiment, the outflow of tracer $^{15}NO_3^-$ was 17% (± 16% SD) lower than predicted by RWT concentrations (Fig. 4A), however ^{15}N abundance, relative to RWT, did not significantly change over time (Fig. 4B) and thus we were unable to calculate a gross uptake rate constant. The $\delta^{15}N$ of NH_4^+ did not increase significantly above background levels during the $^{15}NO_3$ pulse experiment and thus there was no evidence of direct conversion of NO_3^- to NH_4^+ (i.e., by dissimilatory nitrate reduction to ammonium, DNRA). Recoveries of ^{15}N and RWT at the pond outflow were 67% and 85%, respectively.

In the $^{15}NH_4^+$ pulse addition, there was a greater loss of ^{15}N tracer relative to predictions from RWT (Fig. 5A), and we were able to calculate a gross uptake rate constant of 0.11 h^{-1} (± 0.02 SE) (Fig. 5B and Table 2). Gross NH_4^+ uptake was 3.9 mg N m^{-2} h^{-1} and gross NH_4^+ production was 6.2 mg N m^{-2} h^{-1}. Daytime autotrophic uptake of NH_4^+ (13 mg m^{-2} d^{-1}) was sufficient to reduce total NH_4^+ production by 24% (Table 3). There was no detectable increase in the atom percent of ^{15}N of NO_3^- over the course of the pulse addition, and thus nitrification of tracer $^{15}NH_4^+$ was not detectable (although concentrations of NO_3^- were much larger). Recovery of RWT from this pulse experiment was 87%, while recovery of ^{15}N was 23%.

During the steady-state $^{15}NH_4^+$ addition, there were significant declines in $^{15}NH_4^+$ across the pond, which can be related to mean travel times at the various sampling points (Fig. 6). The $^{15}NH_4^+$ uptake rate constant was 0.067 h^{-1} (± 0.019 SE) and did not significantly differ between day and night samplings. Gross NH_4^+ uptake was 8.9 mg N m^{-2} h^{-1} and gross NH_4^+ production was 18.8 mg N m^{-2} h^{-1}. Daytime autotrophic uptake of NH_4^+ (43 mg m^{-2} d^{-1}) was higher than during the $^{15}NH_4^+$ pulse and was sufficient to reduce total NH_4^+ production by 24% (Table 3). However, autotrophic N demand was an order of magnitude greater than autotrophic NH_4^+ uptake (450 mg m^{-2} d^{-1}) and was even twice as high as the gross NH_4^+ uptake (210 mg m^{-2} d^{-1}) (Table 3).

Net uptake of NO_3^- and production of NH_4^+ were principally observed in the shallow upper half of the pond, based on within-pond observations (Table 4). Nitrate concentrations decreased longitudinally along the pond flow path, with most of the NO_3^- lost as water flowed over the shallow mucky delta between Site 1 (1.84 mg N L^{-1}) and Site 4 (1.50 mg N L^{-1}). A majority of the NH_4^+ production occurred over the same reach, with concentrations below detection at the pond inflow and reaching stable concentrations by Site 4. Loss of NO_3^- did not differ between day and night samplings. NH_4^+ production was higher in the night sampling than the day. Concentrations of RWT from the steady-state additions appeared to be stable along the length of the pond in the daytime sampling, but showed a slight decrease along the pond length in the nighttime sampling. Note that the elevated concentrations of RWT and $^{15}NH_4^+$ at Site 2 during plateau 1 reflect a poorly mixed water mass (i.e., a tracer plume). Concentrations of $^{15}NH_4^+$ declined over the length of the pond, and the area of greatest $^{15}NH_4^+$ uptake relative to RWT occurred during the day at Site 3.

Sediment NH_4^+ profiles—Porewater profiles of NH_4^+ and NO_3^- exhibited steep gradients across the sediment–water interface at all three sites within the pond (Fig. 7). Peeper 1 was located near the inflow and had porewater NH_4^+ concentrations of 0.69 mg N L^{-1} just beneath the sediment surface, increasing to 0.90 mg N L^{-1} at 7 cm below the surface. Peeper 2 (located between Sites 2 and 4) and peeper 3 (between Sites 4 and 5) had very high concentrations of NH_4^+ just beneath the sediment surface, 4.3 mg L^{-1} and 4.9 mg L^{-1}, respectively. Nitrate concentrations were below detection limits at all depths below the sediment–water interface. Based on Fick's law and the ponds sediment characteristics, we calculated sediment NH_4^+ fluxes that ranged 33–55 mg m^{-2} d^{-1}. This range is very similar to the net NH_4^+ production observed during the pulsed $^{15}NO_3^-$ (44 mg m^{-2} d^{-1}) and $^{15}NH_3^+$ (42 mg m^{-2} d^{-1}) additions (Table 3).

Denitrification and N_2 : Ar ratios—N_2 : Ar ratios showed a strong diel cycle that differed in the inflow and outflow (Fig. 8A). The magnitude of diel variation was greater at the outflow and the cycle appeared to be temporally offset between inflow and outflow. The model of N_2 : Ar ratios in the pond outflow provided a good fit to the observed pattern (Fig. 8B). Most of the diel variation can be attributed to the water movement through the pond and

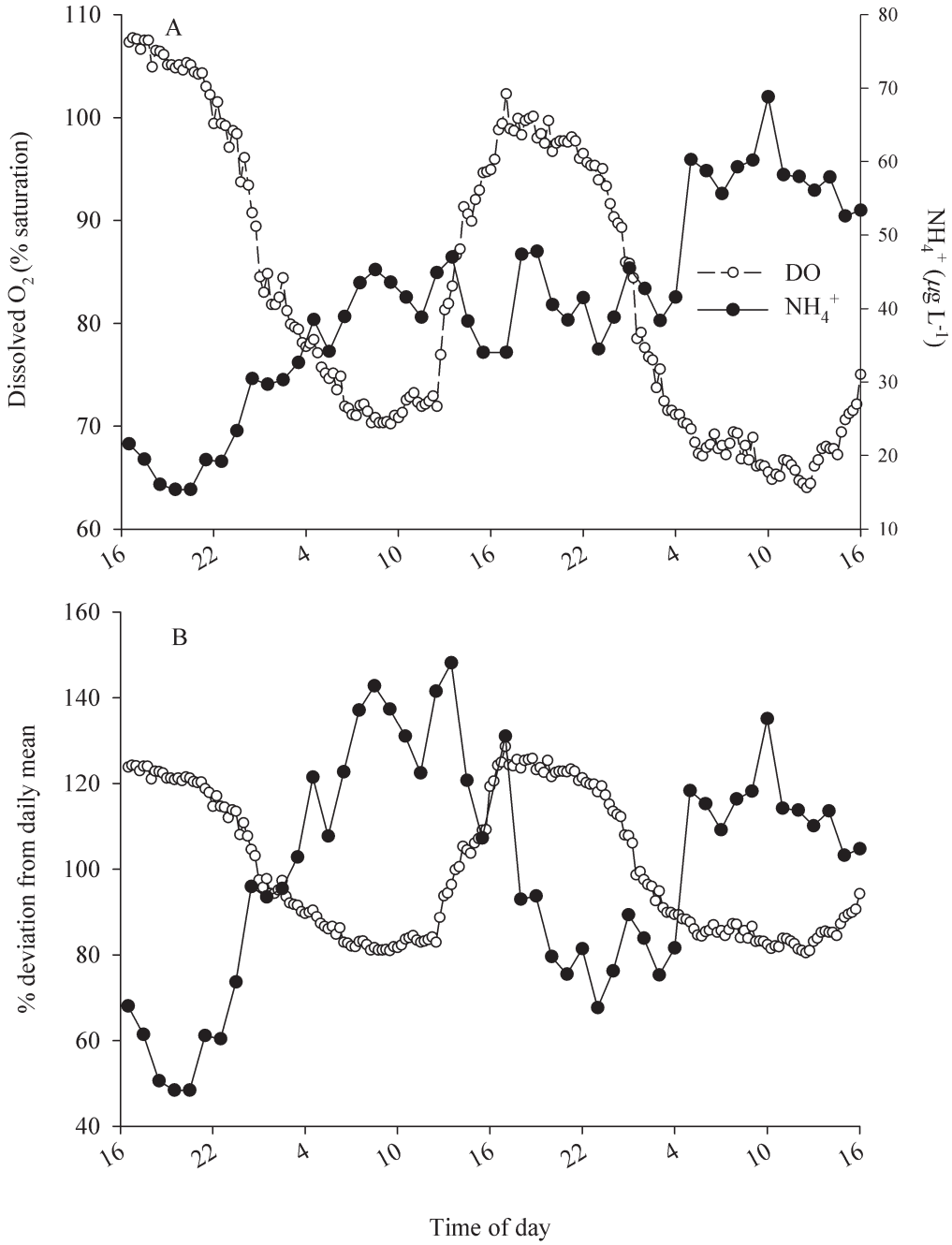

Fig. 3. (A) Diel concentrations of ammonium (NH_4^+) and dissolved oxygen (DO) vary inversely in the pond outflow (05–07 September 2007). (B) When concentrations are standardized as the % of daily means for the trend becomes more evident. Note that there is a 3–4 h time lag due to travel time within the pond and that there is an increasing trend in NH_4^+ and decreasing trend in DO concentrations due to a seasonal effect.

the effects of temperature and gas exchange. The N_2 production (denitrification) term was below the detection limit (i.e., incorporation of denitrification did not improve prediction) when the model was run with a gas-exchange rate of 0.25 h^{-1}, the K_{N2} derived from the diel oxygen curve for the same dates. Similarly, the best fit was achieved with $K_{N2} = 0.14$ h^{-1} and $D_n = 0.00$ mg L^{-1} h^{-1}. In order to account for the effect of uncertainty in gas exchange on the denitrification estimate, we repeated the model fit using the 95% confidence interval estimates of the gas-exchange coefficient (0.06–0.41 h^{-1}) from the night-time O_2 regression approach. The 95% confidence interval for N_2 production in the pond is 0.00–0.05 mg L^{-1} h^{-1}. The upper end of the range of estimated N_2 production would be sufficient to explain the 10% decline in NO_3^- concentrations observed in the pond. It should also be noted that inflow NO_3^- concentrations and water temperature were both lower than during the ^{15}N experiments,

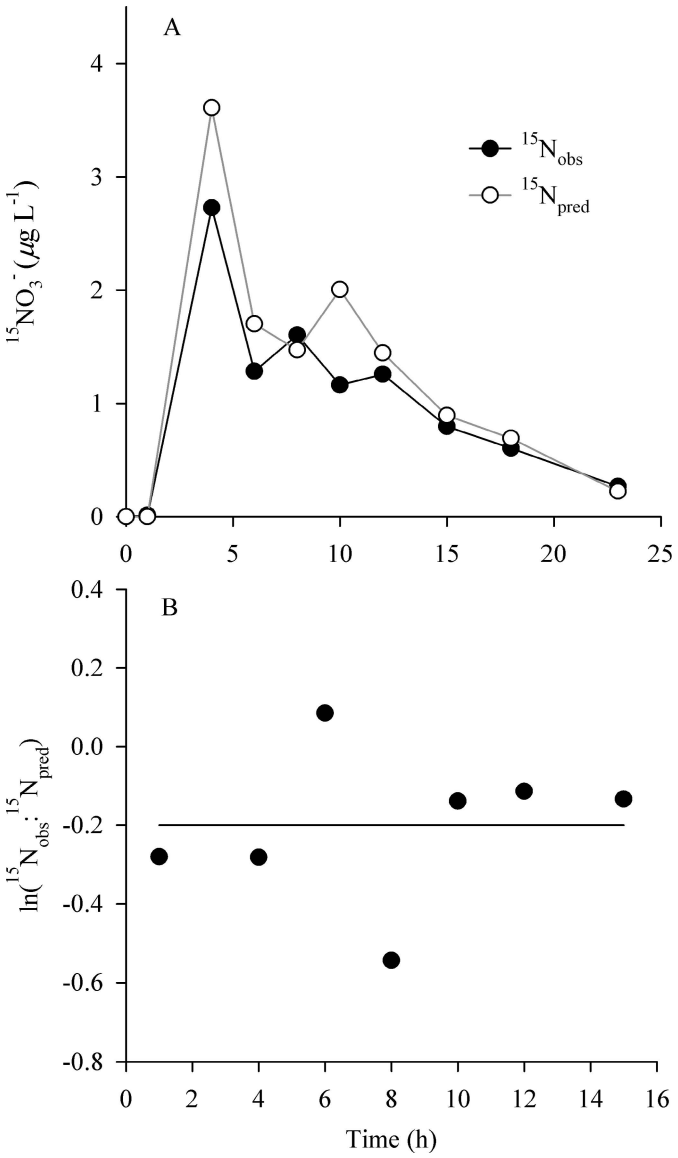

Fig. 4. (A) Predicted and observed abundances of ^{15}N in NO_3^- at the pond outflow following the $^{15}NO_3^-$ pulse addition. (B) There were no significant differences between predicted and observed trends ($^{15}N_{obs}$: $^{15}N_{pred}$) as the pulse moved through the pond, however there was an overall decrease in $^{15}NO_3^-$ relative to RWT.

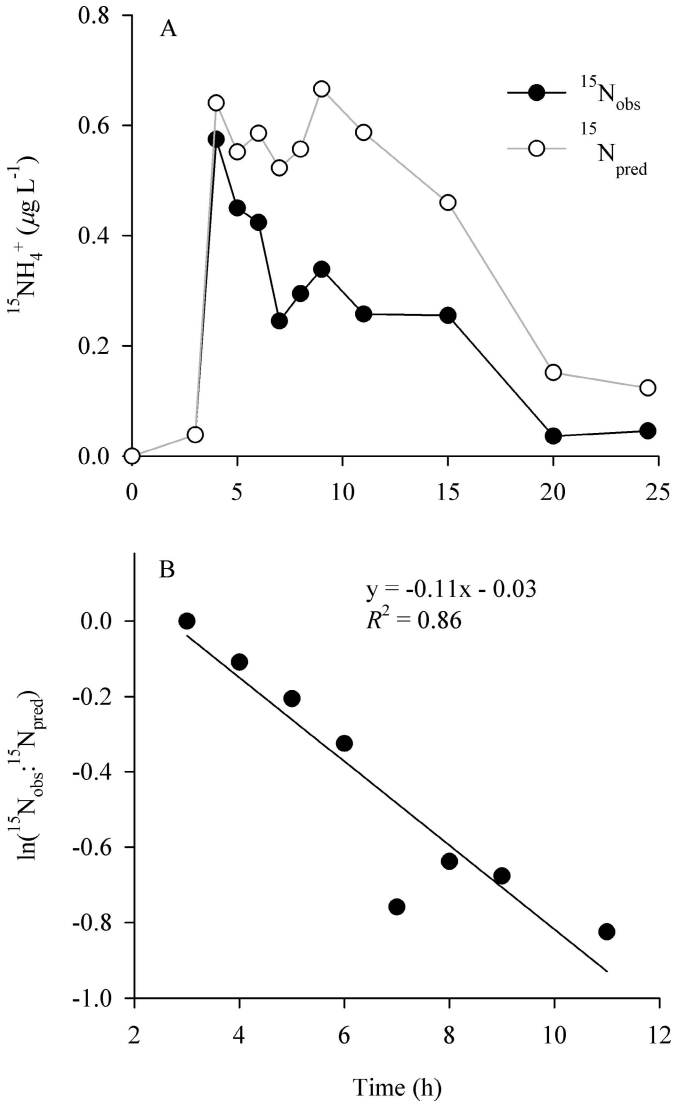

Fig. 5. (A) Predicted and observed concentrations of $^{15}NH_4^+$ at the pond outflow following the $^{15}NH_4^+$ pulse addition. (B) The difference between predicted and observed trends ($^{15}N_{obs}$: $^{15}N_{pred}$) as a function of time was used to calculate the uptake rate constant of 0.11 h^{-1}.

which may have influenced denitrification rates in the pond.

Discussion

In this study we have demonstrated how pulsed additions of $^{15}NH_4^+$ and $^{15}NO_3^-$ can provide insights into the rates and processes of net N uptake or release in a hydraulically complex through-flow wetland. Such experiments helped us to dissect the processes underpinning the 'black box' changes that are observed from input–output comparisons alone. In this case, we determined that sediment NH_4^+ release and autotrophic NH_4^+ assimilation largely controlled net NH_4^+ production, whereas the observed net NO_3^- uptake could be due to denitrification although the evidence from N_2 : Ar measurements does not strongly support this. By performing separate pulsed releases of ^{15}N-labeled NO_3^- and NH_4^+, we can conclude that nitrification did not appear to produce much NO_3^- compared to the concentrations in the through-flowing water, and that there was no evidence for much direct (i.e., dissimilatory) conversion of NO_3^- to NH_4^+ by DNRA. The levels of N transformation and metabolism observed in this pond illustrate the role that through-flow wetlands play as biogeochemical hotspots along landscape flow paths.

Gross $^{15}NO_3^-$ uptake during the $^{15}NO_3^-$ pulse was not significantly different from the net loss of NO_3^- from the water column (Fig. 4B), suggesting that simultaneous production of NO_3^- was not large relative to consumption.

Table 2. Rates of N transformation (± SE) observed during the three ^{15}N addition experiments. Nitrification rates were not detectable (nd) in all three additions.

	$^{15}NO_3^-$ pulse	$^{15}NH_4^+$ pulse	$^{15}NH_4^+$ continuous
^{15}N uptake rate (k_t; h^{-1})	0.00(0)	0.11(0.02)	0.067(0.02)
Gross NO_3^- uptake (mg m^{-2} h^{-1})	15.7(13.4)	—	—
Gross NH_4^+ uptake (mg m^{-2} h^{-1})	—	3.9(1.2)	8.9(3.1)
Gross NH_4^+ production (mg m^{-2} h^{-1})	—	6.2(1.2)	18.8(3.3)
Nitrification (mg m^{-2} h^{-1})	nd	nd	nd
^{15}N recovery (%)	67	23	—
RWT recovery (%)	85	87	—

We observed that a loss of $^{15}NO_3^-$ in the pond (17%) that was not significantly different form the net loss in NO_3^- concentrations (10%). A potential explanation for the decrease in NO_3^- might be dilution by inflowing ground water; however we did not observe a change in discharge between inflow and outflow and we did not see a change in RWT during the steady-state $^{15}NH_4^+$ addition (i.e., there was no change in conservative tracer concentration between the pond inflow and outflow), suggesting no significant groundwater inputs. Samples collected during the steady-state drip did show a strong longitudinal pattern of decreasing NO_3^- concentrations across the pond, where concentrations quickly dropped in the shallow peat delta near the inflow, then remained essentially constant in the deeper portions of the pond. This may explain the lack of pattern in $^{15}NO_3^-$ loss over time. Most NO_3^- uptake from the pulse occurred in the shallowest area near the pond inflow over a short period of time (1–2 h), before water moved into the deeper parts of the pond, where NO_3^- behaved conservatively and spent the majority of its residence time. One explanation for the spatial pattern of NO_3^- loss is that NO_3^- uptake occurred in the upper end of the pond were NH_4^+ concentrations were still low, but further NO_3^- uptake was then blocked by high concentrations of NH_4^+ (the preferred inorganic-N source) in the main portions of the pond.

The maximum estimate of N_2 production was 0.05 mg L^{-1} h^{-1} which corresponds with the magnitude of NO_3^- loss we observed in the pond ($\sim$ 0.45 mg L^{-1} over a travel time of $\sim$ 11 h). However, it is likely that the denitrification rate was lower at the time of N_2 : Ar measurements than during the isotope addition experiments because water temperatures were cooler and NO_3^- concentrations were lower at the pond inflow (11.2°C and 1.10 mg L^{-1} NO_3^- − N) during the N_2 : Ar measurement period due to the arrival of an unseasonal cold front. Despite the ambiguity of this particular denitrification estimate, the methodology itself is promising, although it would benefit from an improved estimate of the gas exchange rate (i.e., K_{N2}).

Net NH_4^+ production in the pond was caused by NH_4^+ diffusing out of the sediments, as evidenced by high concentrations of NH_4^+ in the shallow sediment pore waters. Calculated rates of NH_4^+ diffusion out of the sediments (33–55 mg m^{-2} d^{-1}) were quite similar to the observed net NH_4^+ production in the pond during the pulsed ^{15}N additions (42–44 mg m^{-2} d^{-1}). Elevated NH_4^+ production during the steady-state $^{15}NH_4^+$ addition (194 mg m^{-2} d^{-1}) may be due to the increased mineralization of autochthonous organic matter with the onset of autumn. This increase in NH_4^+ concentrations over time can been seen from the data in Fig. 3A, which was collected in the period between the $^{15}NH_4^+$ pulse and the $^{15}NH_4^+$ steady-state additions. Longitudinal increases in NH_4^+ concentrations within the pond (Table 4) were highest in the shallow areas of the pond where there is the highest ratio of sediment surface area to overlying water volume. It is most likely that particulate organic matter entering the pond from the stream was continuously deposited in the sediments and remineralization of that material produced the high NH_4^+ concentrations in the shallow pore waters and subsequent NH_4^+ export from the pond.

Our results suggest high photoautotrophic NH_4^+ uptake lead to a strong diurnal pattern in NH_4^+ concentrations in

Table 3. Daily net fluxes (± SE) of NO_3^- and NH_4^+ in the pond during the three tracer additions. Net NO_3^- uptake, autotrophic NH_4^+ uptake, net NH_4^+ production, and net NH_4^+ production are based on mass balances from inflow and outflow concentrations. Gross NH_4^+ is based on $^{15}NH_4^+$ additions, extrapolated to a 24-h period. Autotrophic N demand is based on ecosystem metabolism measurement.

	$^{15}NO_3^-$ pulse	$^{15}NH_4^+$ pulse	$^{15}NH_4^+$ continuous
Net NO_3^- uptake (mg m^{-2} d^{-1})	207(70)	115(91)	597(93)
Gross NH_4^+ uptake (mg m^{-2} d^{-1})	—	94(28)	210(74)
Autotrophic NH_4^+ uptake (mg m^{-2} d^{-1})	28(1.3)	13(1.5)	43(5.2)
Autotrophic N demand (mg m^{-2} d^{-1})	320(110)	270(86)	450(120)
Net NH_4^+ production (mg m^{-2} d^{-1})	44(0.8)	42(1.0)	194(4.3)
Total NH_4^+ production (mg m^{-2} d^{-1})	70(6.0)	55(6.0)	237(26)

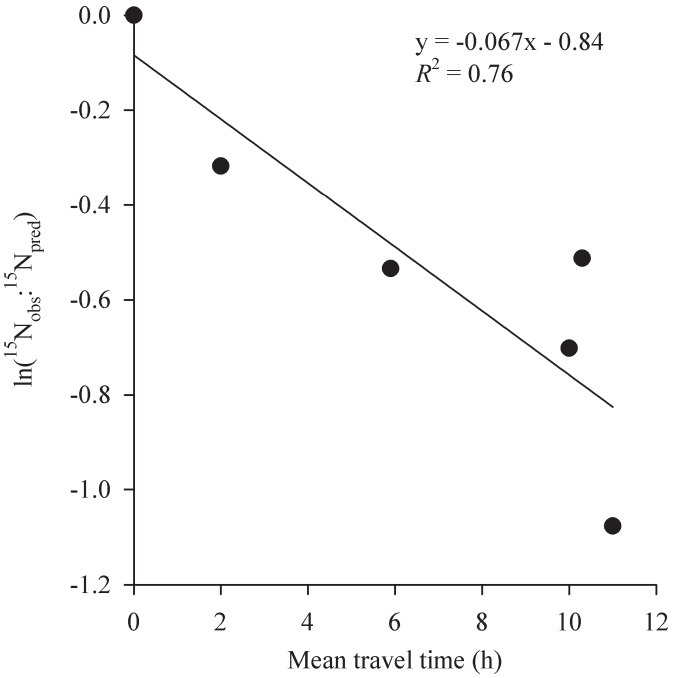

Fig. 6. Uptake of ^{15}N during the continuous $^{15}NH_4^+$ addition, calculated as the change in the abundance of ^{15}N in NH_4^+ relative to the tracer dye at sites within the pond. Mean travel times were estimated from the average travel time of dye to each site.

Table 4. Spatial variation of pond nitrate (NO_3^-), ammonium (NH_4^+), and tracer dye (Rhodamine WT, RWT) concentrations at dawn (24 h) and dusk (36 h) samplings during the continuous $^{15}NH_4^+$ release experiment. Note that Site 1 was at the pond inflow, just up stream of the ^{15}N addition point, and therefore does not have concentrations of added $^{15}NH_4^+$ or RWT.

Site	NO_3^- (mg L−1)	NH_4^+ (μg L−1)	RWT (μg L−1)	$^{15}NH_4^+$ (μg L−1)
Dawn sampling				
1	1.88	0	—	—
2	1.77	46	8.2	0.73
3	1.55	79	6.5	0.32
4	1.49	113	5.7	0.35
5	1.51	101	5.8	0.34
6	1.46	110	5.4	0.27
Dusk sampling				
1	1.84	0	—	—
2	1.78	23	5.7	0.30
3	1.53	36	6.0	0.13
4	1.55	87	6.0	0.30
5	1.54	98	5.9	0.32
6	1.52	79	5.7	0.25

the pond (Fig. 3B), but differences between day and night uptake rates were not evident during the steady-state addition of $^{15}NH_4^+$. This apparent contradiction was because autotrophic NH_4^+ uptake responsible for creating the diurnal cycle only accounted for a small portion of the

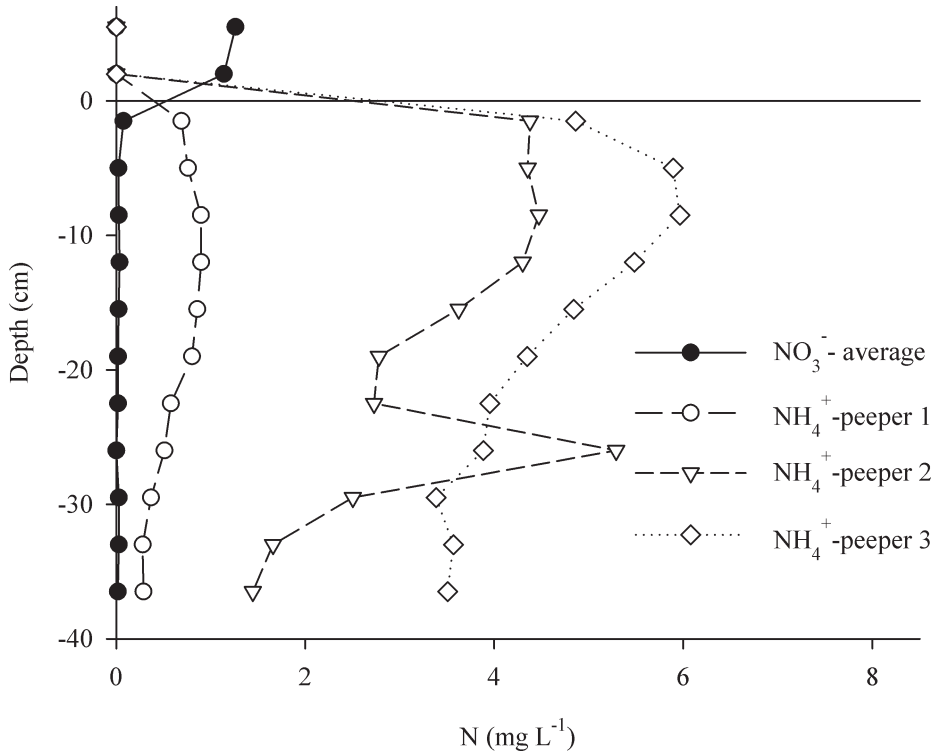

Fig. 7. Porewater concentrations of NH_4^+ (open symbols) and NO_3^- (closed symbols) as indicated by porewater equilibrators at three locations in the pond. High concentrations of NH_4^+ were evident near the sediment surface indicating a net flux to the water column from the sediments.

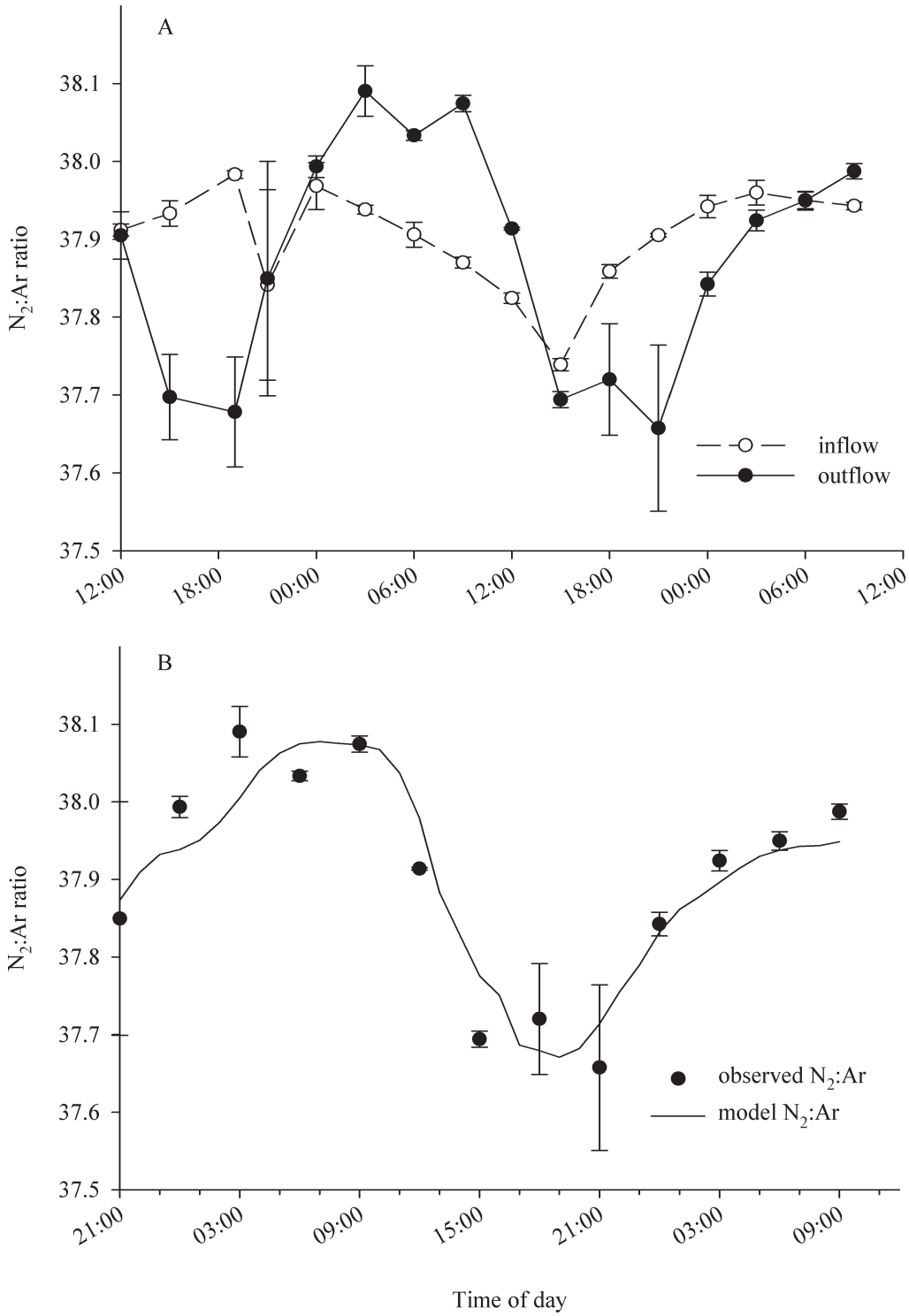

Fig. 8. Ratios of dissolved N_2 : Ar at Kellogg Forest Pond measured from 30 Sepember–02 October 2009. (A) Both the inflow and outflow sites exhibited significant diel fluctuation in N_2 : Ar ratios. (B) Most of the variation in N_2 : Ar at the pond outflow can be explained by the transport and gas exchange within the pond, while denitrification was not significant.

total NH_4^+ uptake. Autotrophic uptake accounted for $< 20\%$ of gross NH_4^+ uptake from both $^{15}NH_4^+$ experiments (Table 3). Moreover, autotrophic demand for N in the pond was an order of magnitude greater than our observed autotrophic NH_4^+ uptake. Much of the photosynthesis was probably due to rooted macrophytes, which have an alternate source of N, namely the high NH_4^+ concentrations in the porewaters. The epiphytes associated

with the macrophytes required N from the water column and are most likely the group of organisms responsible for creating the diurnal cycle in NH_4^+ concentrations.

We did not observe a significant release of reactive phosphorus from the pond, which may have been expected from the net mineralization of organic matter that caused the high NH_4^+ flux. This lack of PO_4^- release from the anoxic sediments is likely due to binding with Fe(III) at the sediment water interface. Iron (III) oxides in the upper sediments may be buffered from reduction by the presence of NO_3^- diffusing in from the water column (Schauser et al. 2006).

Rates of biogeochemical processing in the pond were much higher than in surrounding streams, making this system a biogeochemical hotspot within the surface-water flow path. Rates of aquatic metabolism in Kellogg Forest Pond were much higher than what is typically seen in streams; GPP and CR were well above the upper 1/3 of values for streams (Dodds 2006). CR was more than double the rates reported in nearby Augusta Creek (1.5–3.0 g O_2 m^{-2} d^{-1}; Bott et al. 1985) and Eagle creek (6.4 g O_2 m^{-2} d^{-1}; Hamilton et al. 2001). Similarly, GPP was double that of Augusta Creek (0.5–3.4 g O_2 m^{-2} d^{-1}; Bott et al. 1985) and nearly an order of magnitude higher than Eagle Creek (0.8 g O_2 m^{-2} d^{-1}; Hamilton et al. 2001). Nitrogen processing rates were also high relative to rates observed in streams. Ammonium uptake (32–108 mg m^{-2} d^{-1}) was similar to the range of rates reported in streams (25–330 mg m^{-2} d^{-1}) (Webster et al. 2003), however NH_4^+ production was much higher than rates observed in streams. Nitrate uptake rates (1.2–6.9 μg m^{-2} s^{-1}) were in the upper ranges of the rates reported for a large set of US streams by Mulholland et al. (2008) (median 0.4 μg m^{-2} s^{-1}, upper quartile 1.8 μg m^{-2} s^{-1}), and resulted in a relatively high net uptake rate in the pond compared to many streams.

The pulsed $^{15}NH_4^+$ addition and steady-state $^{15}NH_4^+$ provided comparable measurements of NH_4^+ uptake in the pond. The pulsed isotope additions proved to be a simple and effective technique to measure NO_3^- and NH_4^+ uptake in through-flow systems. The steady-state approach needed 3× as much isotope as the pulsed technique. Similarly the steady-state required six stations spread throughout the pond, whereas the pulsed technique required sampling only at two stations (inflow and outflow). However, the pulsed approach still focused solely on inputs and outputs and largely treats the wetland as a black box. The advantage of the steady-state approach was that it forced us to open the metaphorical black box and take spatially explicit samples to examine where within the pond the biogeochemical processes were happening. We learned new information from this approach (e.g., finding nearly all of the NO_3^- loss was occurring within the 1st 20 m of the pond, similarity between day and night gross NH_4^+ uptake) that later informed our interpretation of the results (i.e., understanding the results of the pulsed ^{15}N additions). In this study, we were able to conduct the steady-state isotope addition only because this pond had a relatively short residence time (11 h). In a larger wetland, with a much longer residence time (> 1–2 d), we would suggest using a pulsed approach rather than a steady-state isotope addition. However, we would still encourage the incorporation of spatially and temporally explicit components into future studies, to examine where and when biogeochemical processes are occurring within the wetland.

In summary, we showed how short-term pulsed ^{15}N tracer additions can elucidate N cycling processes in shallow waters of complex hydrology that are large enough to preclude steady-state tracer approaches. Comparable pulsed additions of ^{15}N-labeled NH_4^+ have been used to examine N cycling in sediments of wastewater treatment wetlands with little standing water (Kadlec et al. 2005), but few studies have examined nontreatment wetlands and employed both $^{15}NO_3^-$ and $^{15}NH_4^+$ tracers. Our experiments showed that this through-flow wetland acted as a sink of NO_3^- and source of NH_4^+. Nitrate was rapidly taken up as it flowed through the wetland with little replacement (i.e., by nitrification). Denitrification estimates were uncertain but may have been sufficient to explain the loss in NO_3^- from the water column. Ammonium was produced by decomposition of organic matter trapped in the wetland, and diffused out of the sediments into the water column. During the day, photoautotrophic production in the wetland mitigated about half of this NH_4^+ export from the sediments. Through-flow wetlands are hotspots of biological activity positioned at key points along landscape flow paths and hence controls on their biogeochemical processes warrant further study. The experiments described here are one promising approach to dissect the wetland black box that has been more typically studied only by mass balances between inflows and outflows.

Acknowledgments

We thank David Weed for assistance with analysis of water samples. Merritt Turetski provided valuable assistance with project development. We also thank two anonymous reviewers for their helpful and insightful comments on the manuscript. This research was funded by a grant from the Michigan State University Center for Water Sciences and from the U.S. National Science Foundation (grants Division of Environmental Biology 0423627 and Division of Environmental Biology 0743402).

References

Alexander, R. B., and others. 2009. Dynamic modeling of nitrogen losses in river networks unravels the coupled effects of hydrological and biogeochemical processes. Biogeochemistry **93:** 91–116, doi:10.1007/s10533-008-9274-8

Aminot, A., D. S. Kirkwood, and R. Kerouel. 1997. Determination of ammonia in seawater by the indophenol-blue method: Evaluation of the ICES NUTS I/C 5 questionnaire. Mar. Chem. **56:** 59–75, doi:10.1016/S0304-4203(96)00080-1

Berner, R. A. 1980. Early diagenesis: A theoretical approach. Princeton Univ. Press.

Böhlke, J. K. 2002. Groundwater recharge and agricultural contamination. Hydrogeol. J. **10:** 153–179, doi:10.1007/s10040-001-0183-3

Bott, T. L., J. T. Brock, C. S. Dunn, R. J. Naiman, R. W. Ovink, and R. C. Petersen. 1985. Benthic community metabolism in four temperate stream systems—an inter-biome comparison and evaluation of the river continuum concept. Hydrobiologia **123:** 3–45, doi:10.1007/BF00006613

Carignan, R., S. St. Pierre, and R. Gachter. 1994. Use of diffusion samplers in oligotrophic lake sediments: Effects of free oxygen in sampler material. Limnol. Oceanogr. **39:** 468–474, doi:10.4319/lo.1994.39.2.0468

Danckwerts, P. V. 1953. Continuous flow systems: Distribution of residence times. Chem. Eng. Sci. **2:** 1–13, doi:10.1016/0009-2509(53)80001-1

Dodds, W. K. 2006. Eutrophication and trophic state in rivers and streams. Limnol. Oceanogr. **51:** 671–680, doi:10.4319/lo.2006.51.1_part_2.0671

———, and others. 2008. Nitrogen cycling and metabolism in the thalweg of a prairie river. J. Geophys. Res. Biogeosci **113:** G04029, doi:10.1029/2008JG000696

Erler, D. V., B. D. Eyre, and L. Davison. 2010. Temporal and spatial variability in the cycling of nitrogen within a constructed wetland: A whole-system stable-isotope-addition experiment. Limnol. Oceanogr. **55:** 1172–1178, doi:10.4319/lo.2010.55.3.1172

Fairchild, G. W., and D. J. Velinsky. 2006. Effects of small ponds on stream water chemistry. Lake Reservoir Manag. **22:** 321–330, doi:10.1080/07438140609354366

Gribsholt, B., and others. 2005. Nitrogen processing in a tidal freshwater marsh: A whole-ecosystem ^{15}N labeling study. Limnol. Oceanogr. **50:** 1945–1959, doi:10.4319/lo.2005.50.6.1945

Groffman, P. M., A. M. Dorsey, and P. M. Mayer. 2005. N processing within geomorphic structures in urban streams. J. N. Am. Benthol. Soc. **24:** 613–625.

Hamilton, S. K., J. L. Tank, D. F. Raikow, W. M. Wollheim, B. J. Peterson, and J. R. Webster. 2001. Nitrogen uptake and transformation in a midwestern US stream: A stable isotope enrichment study. Biogeochemistry **54:** 297–340, doi:10.1023/A:1010635524108

Harrison, J. A., and others. 2009. The regional and global significance of nitrogen removal in lakes and reservoirs. Biogeochemistry **93:** 143–157, doi:10.1007/s10533-008-9272-x

Heffernan, J. B., and M. J. Cohen. 2010. Direct and indirect coupling of productivity and diel nitrate dynamics in a subtropical spring-fed river. Limnol. Oceanogr. **55:** 677–688, doi:10.4319/lo.2009.55.2.0677

Hesslein, R. H. 1976. An in situ sampler for close interval pore water studies. Limnol. Oceanogr. **21:** 912–914, doi:10.4319/lo.1976.21.6.0912

Jansson, M., R. Andersson, H. Berggren, and L. Leonardson. 1994. Wetlands and lakes as nitrogen traps. Ambio **23:** 320–325.

Johnson, C. A., N. E. Detenbeck, and G. J. Niemi. 1990. The cumulative effect of wetlands on water quality and quantity: A landscape approach. Biogeochemistry **10:** 105–141.

Johnson, K. S., L. J. Coletti, and F. P. Chavez. 2006. Diel nitrate cycles observed with in situ sensors predict monthly and annual new production. Deep-Sea Res. Part I **53:** 561–573, doi:10.1016/j.dsr.2005.12.004

Kadlec, R. H., C. C. Tanner, V. M. Hally, and M. M. Gibbs. 2005. Nitrogen spiraling in subsurface-flow constructed wetlands: Implications for treatment response. Ecol. Eng. **25:** 365–381, doi:10.1016/j.ecoleng.2005.06.009

Kana, T. M., C. Darkangelo, M. D. Hunt, J. B. Oldham, G. E. Bennett, and J. C. Cornwell. 1994. Membrane inlet mass-spectrometer for rapid high-precision determination of N_2, O_2, and Ar in environmental water samples. Anal. Chem. **66:** 4166–4170, doi:10.1021/ac00095a009

Laursen, A. E., and S. P. Seitzinger. 2002. Measurement of denitrification in rivers: An integrated, whole reach approach. Hydrobiologia **485:** 67–81, doi:10.1023/A:1021398431995

———, and ———. 2005. Limitations to measuring riverine denitrification at the whole reach scale: Effects of channel geometry, wind velocity, sampling interval, temperature, and inputs of N_2-enriched groundwater. Hydrobiologia **545:** 225–236, doi:10.1007/s10750-005-2743-3

Li, Y. H., and S. Gregory. 1974. Diffusion of ions in sea water and in deep-sea sediments. Geochim. Cosmochim. Acta **38:** 703–714, doi:10.1016/0016-7037(74)90145-8

Lin, A. Y. C., J. F. Debroux, J. A. Cunningham, and M. Reinhard. 2003. Comparison of rhodamine WT and bromide in the determination of hydraulic characteristics of constructed wetlands. Ecol. Eng. **20:** 75–88, doi:10.1016/S0925-8574(03)00005-3

Lightbody, A. F., M. E. Avener, and H. M. Nepf. 2008. Observations of short-circuiting flow paths within a free-surface wetland in Augusta, Georgia, USA. Limnol. Oceanogr. **53:** 1040–1053, doi:10.4319/lo.2008.53.3.1040

Maerki, M., B. Wehrli, C. Dinkel, and B. Muller. 2004. The influence of tortuosity on molecular diffusion in freshwater sediments of high porosity. Geochim. Cosmochim. Acta **68:** 1519–1528, doi:10.1016/j.gca.2003.09.019

Monsen, N. E., J. E. Cloern, L. V. Lucas, and S. G. Monismith. 2002. A comment on the use of flushing time, residence time, and age as transport time scales. Limnol. Oceanogr. **47:** 1545–1553, doi:10.4319/lo.2002.47.5.1545

Mulholland, P. J., H. M. Valett, J. R. Webster, S. A. Thomas, L. W. Cooper, S. K. Hamilton, and B. J. Peterson. 2004. Stream denitrification and total nitrate uptake rates measured using a field ^{15}N tracer addition approach. Limnol. Oceanogr. **49:** 809–820, doi:10.4319/lo.2004.49.3.0809

———, and others. 2008. Stream denitrification across biomes and effects of anthropogenic nitrate loading. Nature **452:** 202–205, doi:10.1038/nature06686

Peterson, B. J., and others. 2001. Control of nitrogen export from watersheds by headwater streams. Science **292:** 86–90, doi:10.1126/science.1056874

Rabalais, N. N. 2002. Nitrogen in aquatic ecosystems. Ambio **31:** 102–112.

Saunders, D. L., and J. Kalff. 2001. Nitrogen retention in wetlands, lakes and rivers. Hydrobiologia **443:** 205–212, doi:10.1023/A:1017506914063

Schauser, I., I. Chorus, and J. Lewandowski. 2006. Effects of nitrate on phosphorus release: Comparison of two Berlin lakes. Acta Hydrochim. Hydrobiol. **34:** 325–332, doi:10.1002/aheh.200500632

Sigman, D. M., M. A. Altabet, R. Michener, D. C. McCorkle, B. Fry, and R. M. Holmes. 1997. Natural abundance-level measurement of nitrogen isotopic composition of oceanic nitrate: An adaptation of the ammonia diffusion method. Mar. Chem. **57:** 227–242, doi:10.1016/S0304-4203(97)00009-1

Seitzinger, S., and others. 2006. Denitrification across landscapes and waterscapes: A synthesis. Ecol. Appl. **16:** 2064–2090, doi:10.1890/1051-0761(2006)016[2064:DALAWA]2.0.CO;2

Stanley, E. H., and A. K. Ward. 1997. Inorganic nitrogen regimes in an Alabama wetland. J. N. Am. Benthol. Soc. **16:** 820–832, doi:10.2307/1468174

Sutton, D. J., Z. J. Kabala, A. Francisco, and D. Vasudevan. 2001. Limitations and potential of commercially available rhodamine WT as a groundwater tracer. Water Resour. Res. **37:** 1641–1656, doi:10.1029/2000WR900295

Tobias, C. R., M. Cieri, B. J. Peterson, L. A. Deegan, J. Vallino, and J. Hughes. 2003. Processing watershed-derived nitrogen in a well-flushed New England estuary. Limnol. Oceanogr. **48:** 1766–1778, doi:10.4319/lo.2003.48.5.1766

Young, R. G., and A. D. Huryn. 1999. Effects of land use on stream metabolism and organic matter turnover. Ecol. Appl. **9:** 1359–1376, doi:10.1890/1051-0761(1999)009[1359:EOLUOS]2.0.CO;2

Webster, J. R., and others. 2003. Factors affecting ammonium uptake in streams—an inter-biome perspective. Freshw. Biol. **48:** 1329–1352, doi:10.1046/j.1365-2427.2003.01094.x

Zedler, J. B. 2003. Wetlands at your service: Reducing impacts of agriculture at the watershed scale. Front. Ecol. Environ. **1:** 65–72, doi:10.1890/1540-9295(2003)001[0065:WAYSRI]2.0.CO;2

Associate editor: George W. Kling

Received: 12 November 2010
Accepted: 17 August 2011
Amended: 13 September 2011